Brick versus shell elements in simulations of aluminium extrusions subjected to axial crushing

Ø. Fyllingen[a], O.S. Hopperstad[b], A.G. Hanssen[b], M. Langseth[b]

[a] Department of Civil Engineering, Bergen University College, NO-5020 Bergen, Norway

[b] Structural Impact Laboratory (SIMLab), A Centre for Research-based Innovation (CRI), Department of Structural Engineering, Norwegian University of Science and Technology, NO-7491 Trondheim, Norway

Summary: In previous published literature, deviations in the mean crushing force and deformation pattern have been found between simulations with plane stress shell elements and experimental results for aluminium extrusions subjected to axial crushing. In the current study, simulations with solid and shell element models were carried out and compared to experimental results to study the influence of element type for this class of problems. The mean crushing force in the simulations using shell elements with through thickness stretch and solid elements were much closer to the experimental values than the plane stress shell elements. Concerning the deformation pattern, the solid element simulation exhibited a folding pattern much closer to the experimental one than the simulation with plane stress shell elements. To validate the conclusions drawn here, simulations of profiles with other geometries should be performed and compared to experimental results.

Keywords: Brick and shell elements, aluminium extrusion, structural impact, finite element method
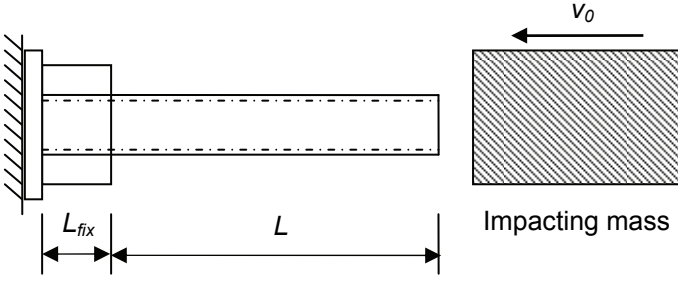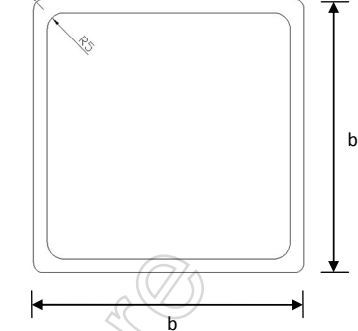
1   Introduction

Thin-walled structures are used as energy dissipating structures in a car. Normally, these structures are modelled by use of plane stress shell elements. In general, reasonable agreement between shell based finite element simulations and experimental results is found in the literature. However, several investigations involving both experimental tests and shell based simulations of extruded aluminium profiles have pointed out that the predicted mean crushing force is generally underestimated (e.g. Jensen et al. [1] and Reyes et al. [2]). Compared to steel sections, the extruded aluminium sections typically have a larger wall thickness in order to compensate for the lower strength.

One explanation for the underestimated mean crushing force is that plane stress shell elements are not adequate for modelling of extruded aluminium profiles. In the current study, simulations with solid and shell element models will first be carried out to investigate the influence of element type on the predicted axial crushing behaviour of extruded aluminium profiles. Then, a comparison to experimental results will be performed. Until recently, the computers have not been fast enough and the memory has been too small to perform proper simulations with solid elements of such profiles. It is still not possible to carry out adequate full-scale crash simulations with only solid elements, but smaller problems might be modelled by use of solid elements and compared to models with shell elements.

2   Experimental set-up

The simulations are based on experiments performed by Jensen et al. [3]. A short description of the test set-up is given here. Jensen et al. [3] tested extruded profiles of aluminium alloy 6060 T6 subjected to axial crushing. Profiles of different lengths and thicknesses were subjected to impact at different velocities. In the current study, the focus will only be on profiles with 2.5 mm thickness and 20 m/s impact velocity. The test set-up and the geometry of the cross section is presented in Table 1.

Table 1. Test specimen geometry and support conditions for the dynamic tests (Jensen et al. [3]).

Test set-up	Cross section
Dynamic	

The extrusion had a square-shaped cross section with a width (*b*) of 80 mm. The corners were slightly rounded with inner radius 5 mm and outer radius 3 mm. The free length of the profiles (*L*) varied between 639 mm and 1600 mm. A pendulum accelerator was used to accelerate the impacting mass of 600 kg up to an initial velocity (*v₀*) of 20 m/s, hitting the free end of the specimens. At the distal end, the specimens had a clamped support. The length of this support was 100 mm.

3 Simulations

In this section, the simulations will be described. As mentioned in the introduction, simulations with brick elements are quite time consuming. Hence, it was chosen to first perform a convergence study on a short profile to see how many brick elements are necessary through the thickness to obtain satisfactory results, see section 3.1. Based on the results from section 3.1, simulations of a longer profile are performed and compared to the experimental results in section 3.2.

3.1 Simple model

It was chosen to have a length such a length of 200 mm. The impacting mass was modelled by attaching a row of elements with rigid body material, total mass of 600 kg and initial velocity of 20 m/s to the profile. Concerning the nodes in the fixed end, all the degrees of freedom were fixed. The von Mises yield function and a piecewise linear hardening description of the extended Voce rule with 0.5 % strain increments were chosen. The hardening was based on coefficients for the extended Voce rule found by Jensen et al. [3]. The density was set to 2700 kg/m³, the Young's modulus was 70 000 MPa and the Poisson's ratio was 0.3.

Based on previous studies by Fyllingen et al. [4], these simulations are known to be very sensitive to small changes, such as geometric imperfections and small changes in the material description. Hence, in the convergence study it was chosen to use geometrical triggers to ensure that the first lobe develops at the same place in all the simulations.

An imperfection field, which forms a half sine wave across the width of the profile and is uniform in the extrusion direction, was used to trigger the deformation mode, see Figure 1 (a). The amplitude of the imperfection was *b*/200. In addition, the top 50 mm was triggered; see Figure 1 (b). The trigger consists of a product of trigonometric waves. In the width direction, a half sine wavelength is applied. In the axial direction, one sine wavelength is used. The trigger points outwards on two of the parallel walls and inwards on the remaining two parallel walls. The maximum amplitude was *b*/100. The trigger amplitude is added to the imperfections applied for the whole extrusion length.
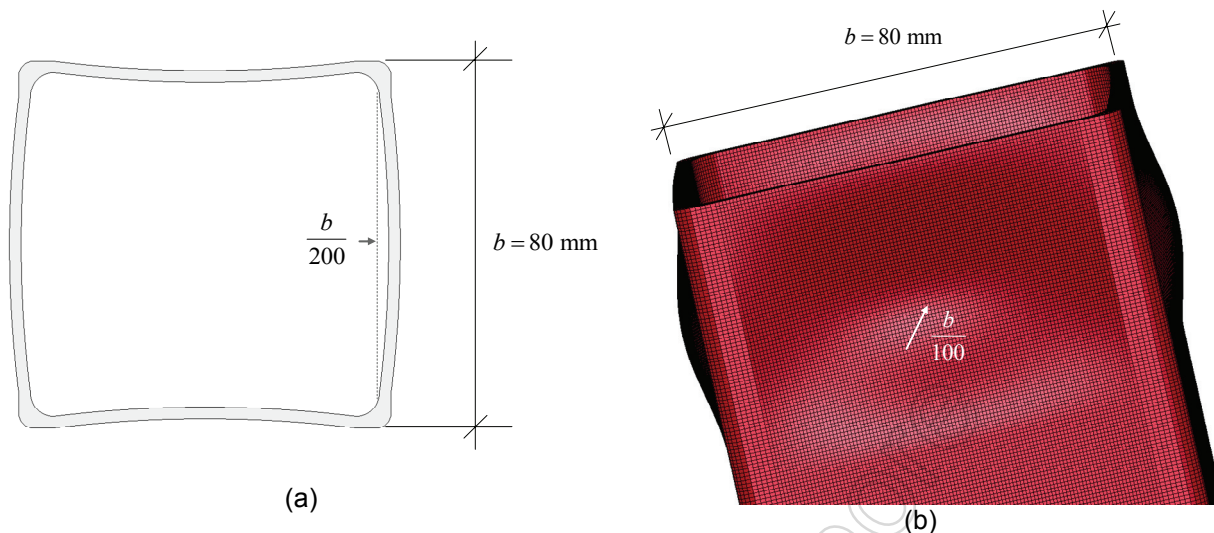
(a)

(b)

Figure 1. (a) Cross-section with amplified imperfections; (b) Illustration of trigger

It was chosen to test two different types of shell formulations and one of the brick formulations implemented in LS-DYNA (Hallquist [5]). In a pre-study, comparisons between the Belytschko-Tsay type shell elements and their corresponding fully integrated shell formulations were performed, resulting in very similar results. Hence, the fastest formulations were chosen. The two shell formulations chosen are the Belytschko-Tsay shell (shell type 2) and the Belytschko-Tsay shell with through thickness stretch (shell type 25). Jensen [6] performed a convergence study and found that 20 shell elements over the width were satisfactory. However, it was chosen to use as small elements as possible and still be able to have a contact thickness equal to the true thickness. Hence, it was possible to have square-shaped elements with a size of 2.5 mm, resulting in about 30 elements over the width.

Concerning the solid elements, it was chosen to use the fully integrated S/R element (solid type 2). In order to check the convergence for the solid model, it was modelled with 1, 2, 3, 4 and 6 approximately cube-shaped elements through the thickness. The self-contact type chosen in LS-DYNA was "*CONTACT_SINGLE_SURFACE" with zero friction (Hallquist [5]).

In Figure 2 (a), the force-displacement curves for the solid element simulations are shown. The simulations with 1 and 2 elements through the thickness deviate somewhat from the rest. The simulations with 3 or more elements through the thickness give similar results, and hence it should be sufficient with 3 elements through the thickness to obtain a solution close to the converged force-displacement curve.

The resulting force-displacement curves using shell element type 2 and 25 and solid element type 2 with 6 elements through the thickness are plotted in Figure 2 (b). Both shell element simulations follow the solid element simulation quite well somewhat beyond peak load. For larger deformations the three curves deviate. The mean crushing force evaluated for a deformation up to 120 mm are 62.9 kN, 51.3 kN and 59.1 kN for solid type 2, shell type 2 and shell type 25, respectively. Hence, there are especially large deviations between the solid element and plane stress shell element simulations.
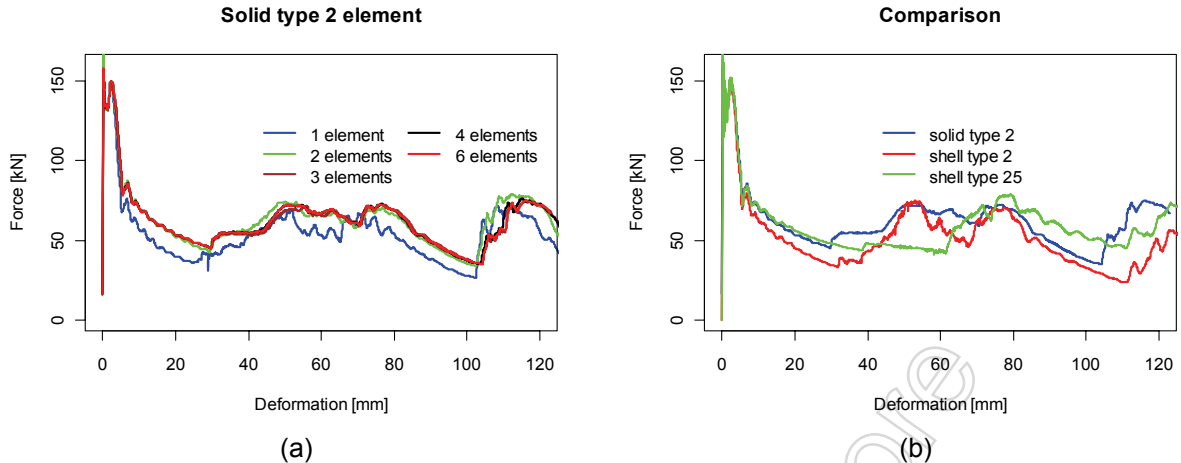
Solid type 2 element

Comparison

Figure 2. Force displacement curves: (a) Solid element; (b) Comparison shell and solid elements

In Figure 3, pictures of the deformed geometry for all three simulations are given. As can be seen, the same number of lobes developed for all the simulations, but the shape of the lobes differs. The differences will be more apparent in the next section, where the length of the profile is increased.
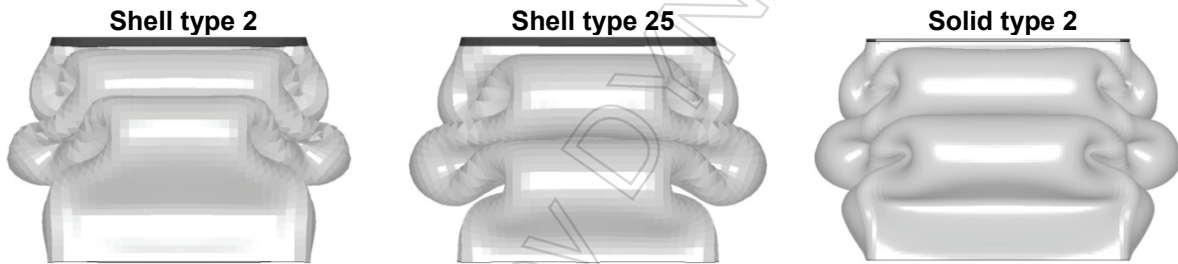
Shell type 2   **Shell type 25**   **Solid type 2**

Figure 3. Pictures of the deformed geometry

3.2 Model of the experiment

The solid element simulations performed in the previous section were quite time consuming. Hence, it was chosen to model the shortest section tested by Jensen et al. [3]. This profile had a free length of 639 mm. The profiles used in the experiments did not have any geometrical trigger. However, Jensen et al. [1] experienced difficulties to obtain the correct buckling pattern without the imperfections along the walls. Hence, the imperfection along the walls was still kept, while the trigger at the top 50 mm was removed from the model. Based on the results from the previous section, a mesh with 3 solid elements through the thickness was chosen. The size of the shell elements was still 2.5 mm.
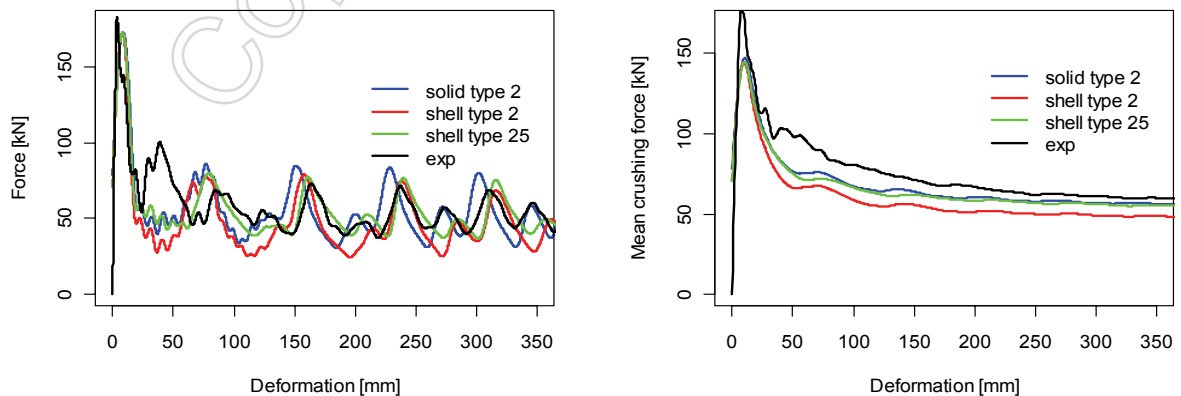
Figure 4. (a) Force versus deformation; (b) Mean force versus deformation

In Figure 4 (a), the force-displacement curves are given for the two shell element simulations, the solid element simulation and the experiment (exp). The position of the second peak is quite similar for all the simulations, while the position of the second peak in the experiment differs from the simulations. The lobes start to develop at the fixed end and propagate towards the free end in all the simulations and the experiment. The observed deviation in the second peak can be explained by looking at the deformed geometries, see Figure 5. The lobes nearest the fixed end (uppermost edge in the pictures) in the experiment differ from the corresponding lobes in the simulations. One explanation for the deviation might be that the profile is not entirely fixed at the distal end. Instead, there is a fixation device with a length of 100 mm. However, Jensen et al. [3] experienced a lot of variation in how the first lobes developed in the experiments. By comparing the simulations and the experiment at the stage beyond the second peak, it seems like the simulations with shell type 25 give quite reasonable results. Also the solid element model is not far from the experimental curve, except for phase shift. The curve for the shell type 2 has much lower valleys than the experimental curve. By comparing the last lobes developed, see Figure 5, it seems like especially good agreement is found between the solid type 2 model and the experiments.
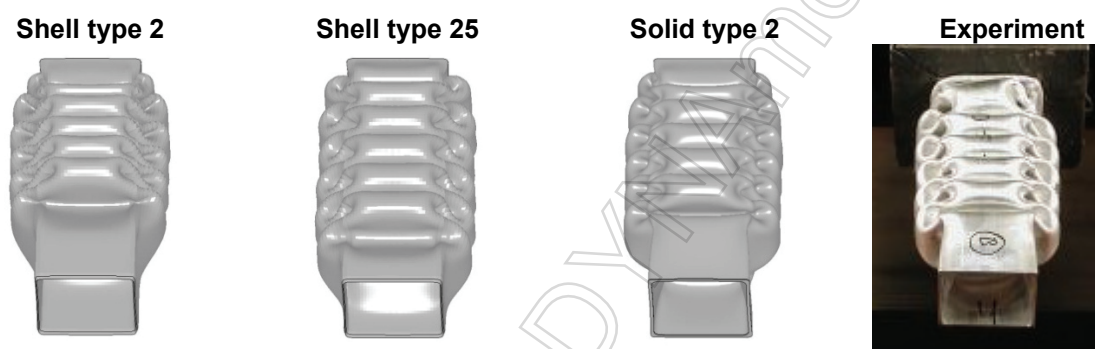

Figure 5. Geometry at approximately same deformation

The mean crushing force versus deformation is plotted in Figure 4 (b). For low deformations the mean crushing force is underestimated in all the simulations compared to the experiments. This can be explained by how the first lobes develop. As the deformation increases, the mean crushing force for shell type 25 and solid type 2 approaches the experimental value. For a deformation of 368 mm, the mean crushing forces are 48.2 kN, 55.4 kN, 56.0 kN and 59.4 kN for the shell type 2, shell type 25, brick type 2 and experiment, respectively.

4   Discussion and concluding remarks

The objective of the study was to investigate whether the large differences between simulations and experiments in axial crushing of aluminium extrusions could be due to the plane stress shell elements. From the investigation performed here, it seems like the force level is more similar to the experimental one in simulations with solid elements and shell elements with through thickness stretch compared to simulations with plane stress shell elements. By comparing the deformed geometries, good agreement is found between the solid element simulation and the experiment, while large deviations were obvious between the plane stress shell simulation and the experiment. In the models, several simplifications are introduced and also the material model is quite simple. Hence, some deviations between the simulations and experiments should be expected. Further studies comparing simulations to several experiments should be performed in the future to investigate whether the differences observed here are also valid for aluminium extrusions with other geometries.

From an industrial point of view, it is difficult to run solid element simulations for large scale problems because of the simulation time. It seems like the shell with through thickness stretch gives better results than the plane stress shell. Hence, shell type 25 could be a good alternative for use in large scale simulations. Of course, also here, further validation is necessary to see if this element performs well for other types of geometries.

5   References

[1] Jensen Ø., Hopperstad O.S., Langseth M., Transition from progressive to global buckling of aluminium extrusions – a numerical study, IJCrash 10 (2005) 609-620.

[2] Reyes A., Langseth M., Hopperstad O.S., Crashworthiness of aluminum extrusions subjected to oblique loading: experiments and numerical analyses, International Journal of Mechanical Sciences 44 (2002) 1965–1984.

[3] Jensen Ø, Langseth M, Hopperstad OS. Experimental investigations on the behaviour of short to long square aluminium tubes subjected to axial loading. International Journal of Impact Engineering 30 (2004) 973-1003.

[4] Fyllingen Ø, Hopperstad O.S., Langseth M., Stochastic simulations of square aluminium tubes subjected to axial loading, International Journal of Impact Engineering 34 (2007) 1619-1636.

[5] Hallquist JO. LS-DYNA Keyword User's Manual, Version 970, Livermore Software Technology Corporation, 2003.

[6] Jensen Ø., Behaviour of aluminium extrusion subjected to axial loading, Doctoral Thesis at the Norwegian University of Science and Technology, (2005).